

## Localization and Nonlinear Resistance in Telescopically Extended Nanotubes

John Cumings\* and A. Zettl†

Department of Physics, University of California at Berkeley and Materials Sciences Division, Lawrence Berkeley National Laboratory, Berkeley, California, 94720, USA

(Received 24 February 2004; published 18 August 2004)

We have measured the electrical resistance  $R$  between the ends of a multiwall carbon nanotube during telescopic extension of the nanotube.  $R$  increases monotonically with extension and is hysteresis free, demonstrating that a telescoping nanotube constitutes a near-ideal nanometer-scale rheostat. The functional form of  $R$  is nonlinear and consistent with an exponential form predicted for a one-dimensional localized system, with a characteristic localization length 1000–1500 nm.

DOI: 10.1103/PhysRevLett.93.086801

PACS numbers: 73.63.-b, 73.23.-b

The study of carbon nanotube electronic transport is an active experimental and theoretical research area. It has been demonstrated that single-walled carbon nanotubes (SWNTs) are physical realizations of ideal quantum wires with ballistic conduction [1–3]. Electronic conduction through multiwall carbon nanotubes (MWNTs), on the other hand, is complicated by intershell interactions and possible wave function interference between electronic states on different shells of the composite tube. For charge transport in such MWNTs the experimental understanding is complicated, with different studies variously supporting quantized electrical conductance, conductance dominated by transport along the outermost shell, diffusive scattering, and current-induced damage [2,4–8]. Part of the difficulty is that most transport experiments are performed without detailed knowledge of the MWNT geometrical characteristics as might be obtained via high-resolution transmission electron microscopy (TEM).

Recently, it was demonstrated that the core shells of MWNTs could be controllably telescoped from their outer shell housings, thus constituting low-friction linear bearings [8–10]. Such experiments were performed *in-situ* inside a high-resolution TEM, allowing simultaneous imaging of the MWNT system. An interesting measurement enabled by this geometry is the determination of the electrical resistance  $R$  between the ends of a telescoped MWNT as the telescoping distance,  $x$ , is varied. In this Letter, we report on the results of such measurements. For all nanotubes studied,  $R$  is found to increase nonlinearly with increasing  $x$ . The functional form of  $R(x)$  and the electric field dependence of  $R$  are consistent with predictions for a one-dimensional localized system, with a room-temperature carrier localization length 1000–1500 nm.  $R(x)$  is highly reproducible, suggesting that telescoped MWNTs constitute reliable high-resolution nanoscale rheostats.

The experimental starting point was with MWNTs whose core tubes had been partially exposed and mechanically contacted using methods previously described

[8,9]. Briefly, one end of a bundle of surfactant-free (i.e., unprocessed) arc-grown MWNTs was embedded in silver paint and attached to a stationary electrode. The furthest protruding nanotube was peeled open by current-induced damage and the protruding core tubes were contacted via spot-welding to a piezo driven nanomanipulator electrode. During the experiment, the dc electrical resistance between the two electrodes was monitored as the nanomanipulator (reversibly) telescoped the inner core tubes out from, or collapsed them back into, the outer nanotube housing.

Figure 1 shows schematically the experimental configuration. The telescoping or extraction distance  $x$  was monitored both via the nanomanipulator piezo drive voltages and analysis of direct TEM video recordings of the telescoping process. Typical MWNT initial (i.e., fully collapsed) lengths were from one to several microns. The nanotube system was always suspended in high vacuum inside the TEM (Topcon 002B, operating at 100 keV), thus eliminating potentially spurious substrate effects.

Figure 2 shows, for three independent MWNTs labeled A, B, and C, the resistance  $R$  between the ends of the telescoping nanotube system as a function of telescoping or core extraction distance  $x$ . The solid symbol data points have been normalized to  $R_0$ , the resistance of the  $x \rightarrow 0$  unextended MWNT. The values of  $R_0$  ranged from 3.5 to 110 k $\Omega$ . Data such as those shown in Fig. 2 were recorded for successive extension and contraction runs and were

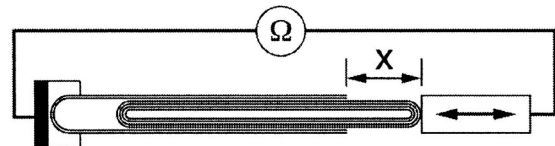


FIG. 1. Schematic diagram of telescoped MWNT resistance measurements. On the left is a nanotube anchored inside the TEM, and on the right is the manipulation tip. The nanotube is reversibly telescoped while the dc electrical resistance is measured with a low noise current amplifier.

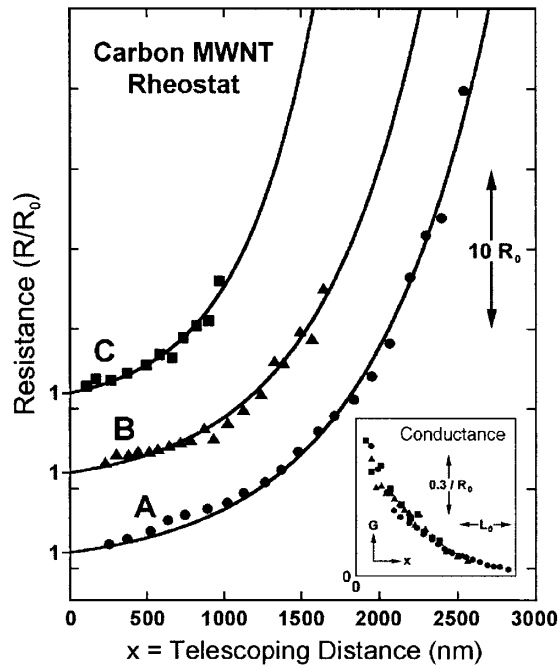


FIG. 2. Resistance  $R$  vs telescoping distance ( $x$ ) for three different nanotubes. The data are normalized to  $R_0 = R(x \rightarrow 0)$ . The inset shows the same data plotted as conductance ( $1/R$ ) as a function of normalized telescoping distance ( $x/L_0$ ). Note that the conductance data are also nonlinear and collapse onto a universal curve.

found to be reproducible without evidence of significant hysteresis or temporal drift. The reproducibility of the devices indicates that the 100 keV imaging electron beam of the TEM does not cause significant structural damage to the nanotubes during the measurements.

The resistance data of Fig. 2 are clearly not linear in telescopic extension. To fit the data to a nonlinear functional form, we choose

$$R(x) = R_0 \exp(x/L_0), \quad (1)$$

with  $L_0$  a characteristic length to which we attach a physical meaning below. The solid lines in Fig. 2 are fits of Eq. (1) to the three experimental  $R(x)$  data sets. Fitting parameters for the three curves are given in Table I, along with other relevant nanotube parameters obtained via TEM imaging. The inset of Fig. 2 shows the same data plotted as conductance,  $G(x) = 1/R(x)$ , as a function of the normalized telescoping distance,  $x/L_0$ ; the conductance also exhibits nonlinearity with positive second derivative. From this observation and simple calculus manipulations we can rule out various functional forms for  $R(x)$ : any series combination of linearly changing resistance or conductance, any logarithmic dependence, or any power law,  $R(x) \propto x^\alpha$ , where  $\alpha \leq 1$ . Functional forms that are consistent with this observation include an exponential functional form, such as Eq. (1), or a power law with  $\alpha > 1$ .

TABLE I. The sizes of the nanotubes reported here, and the parameters extracted from the fits to the data shown in Fig. 2. The nanotube core section inner diameters are not given as they could not be unambiguously resolved from the microscopy images, but from observations of other nanotubes in our sample the inner diameters are typically 1–3 nm.

Nanotube	Housing Outer Diameter	Core Outer Diameter	Core Length	$R_0$	$L_0$
A	25 nm	18 nm	2.6 $\mu\text{m}$	3.5 k $\Omega$	760 nm
B	18 nm	7 nm	1.7 $\mu\text{m}$	54 k $\Omega$	670 nm
C	20 nm	5 nm	1.1 $\mu\text{m}$	110 k $\Omega$	490 nm

We now discuss these experimental findings. We first examine two candidate models for the resistance behavior: diffusive transport and junction tunneling. In the (semiclassical) diffusive transport model the increase in resistance with telescoping results from strictly geometric considerations. Two hollow and concentric, tightly fitting metal cylinders can show an increasing  $R$  that is not strictly linear with increasing telescoping distance  $x$ . Even assuming an isotropic conductivity tensor, this model is difficult to solve exactly, but, in the limit of very thin cylinder walls or very long telescoping distances (as we have for the MWNT system), the model predicts a linear increase in  $R$  with increasing  $x$ . Under no circumstances does the generalized model yield the observed unique nonlinear length dependence.

In the junction tunneling model, the dominant contribution to the resistance arises from charge carriers tunneling from the telescoped nanotube core to the nanotube housing, while along the core and housing regions themselves the charge transport is assumed ballistic with no inherent length dependence to the resistance. A tunneling probability proportional to the core/housing overlap area then leads to a linear decrease in *conductance*,  $1/R(x)$ , with increasing  $x$ . The inset of Fig. 2 clearly shows that the conductance also decreases nonlinearly, ruling out this possible explanation. Indeed, our data suggest that the conductance of the sliding contact between the nanotube core and its housing is actually quite good, in agreement with independent experimental [11] and theoretical [12] studies. The addition of a contact resistance to the junction tunneling model does not improve the fit to the experimental conductance data (this would cause a functional form with negative second derivative).

We propose that the correct interpretation of the observed nonlinear  $R(x)$  is on-tube quantum interference and localization of electron wave functions similar to that first proposed by Landauer and Thouless for low-dimensional systems with defect scattering [13]. In the original localization model of Landauer, a one-

dimensional conduction channel has a distribution of scattering sites, and the effect of increasing the length of the channel is to cause a linear increase in the number of scatters in the path of the transport current. Because of quantum interference, however, each scatterer introduces a multiplicative factor in the averaged total system resistance, resulting in a resistance that increases exponentially with the length  $x$  of the system. Thouless later showed that the prediction also holds for a three-dimensional conducting wire with many channels, provided that, among other conditions, the wave functions of the carriers are phase coherent across the diameter of the wire. The localization model also predicts an exponential dependence of resistance on temperature. While the signature of localization in the temperature dependence of resistance has been experimentally verified for a host of low-dimensional systems, including carbon nanotubes and graphitic materials [14], the unambiguous observation of an exponential length dependence of the resistance of a localized system has remained experimentally elusive [15].

The critical parameter in the localization model is the localization length  $l_c$ , representing the probability amplitude decay length of the (nonextended) electronic wave functions. For a two-terminal resistance measurement as employed for our telescoped MWNT system, the total resistance can be expressed within the localization model as [16]

$$R(x) = R_0[\exp(2x/l_c - 1)] + R_c, \quad (2)$$

with  $R_c$  the resistance of the fully collapsed nanotube. With the substitutions  $l_c = 2L_0$  and  $R_0 = R_c$ , Eq. (2) is in fact identical to Eq. (1). From our previous fits in Fig. 2 we find that the localization length  $l_c$  ranges approximately from 1000 to 1500 nm in the telescoped MWNT systems here investigated (see Table I). The correspondence between the scaling factor  $R_0$  and the collapsed tube “contact resistance”  $R_c$  suggests that  $R_c$  enters into the MWNT localization problem in the same way as do the intrinsic scattering sites, namely, as a multiplicative factor.

Localization theory makes additional, experimentally testable predictions concerning the electric field  $E$  dependence of the electrical resistance [17]. For low applied  $E$ , Ohmic conduction should be observed, while for high applied  $E$ , the range of accessible states is increased leading to nonlinear conductance. The different field regimes can be characterized by the parameter [17]

$$\beta = eEl_c/2k_B T, \quad (3)$$

where  $e$  is the electron charge,  $k_B$  is Boltzmann’s constant, and  $T$  is the absolute temperature. For  $\beta \ll 1$ , transport is dominated by thermally assisted hopping, while for  $\beta \gg 1$ , transport is dominated by field-induced hopping. We have measured the electric field dependence of the telescoped MWNT system, as shown in Fig. 3 for

nanotube  $B$  at a fixed telescopic extension. At low applied voltages the resistance is approximately constant with some fluctuations due to experimental noise. At high applied voltages, however, the resistance decreases precipitously with increasing voltage. The vertical dashed line in Fig. 3 corresponds to  $\beta = 1$ , calculated using  $l_c = 1340$  nm as determined from the  $R(x)$  fit for nanotube  $B$ . This demarcation agrees well with the observed transition from Ohmic to strongly nonlinear resistance, providing additional support for carrier localization.

What is the origin of the “disorder” leading to carrier scattering and localization in the telescoped nanotube system? We cannot answer this question directly with our results alone, but we shall outline our understanding of the question and give some possible sources of the disorder. In order to address this question, we shall first attempt to determine the mean free path of charge carriers in our nanotube structures. In localization theory, the localization length is connected with the disorder-determined mean free path,  $l_e$ , and the number of parallel conduction channels,  $M$ , through the relationship  $l_c = Ml_e$ . In the determination of  $M$ , we note that low-temperature studies conclude that all current in MWNTs is carried only in the outermost nanotube layer [4], but more recent room-temperature studies present evidence that transport current probes more than one nanotube shell [11]. For typical nanotubes at room-temperature, it has been suggested that approximately 3–7 shells contribute significantly to the current in pristine MWNTs. Furthermore, in our structures, the current must traverse approximately 10–20 nanotube layers to get from the outer layer of the housing to the outer layer of the core. From this, we estimate that  $M$  could reasonably be in

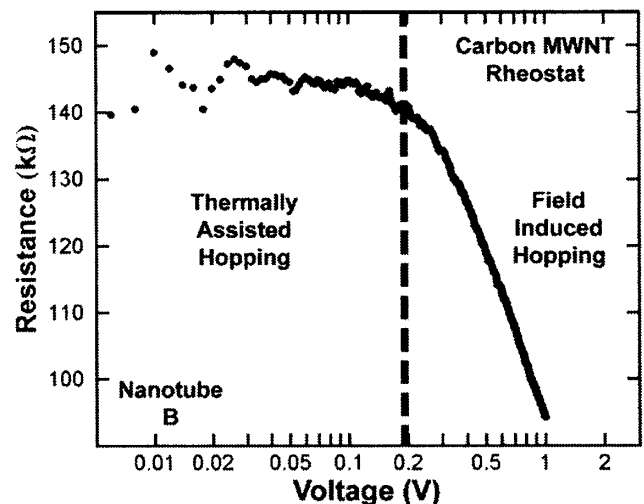


FIG. 3. Resistance vs applied voltage of nanotube  $B$  when it is telescoped at a distance of  $x = 580$  nm. The vertical dashed line is the calculated delineation between thermally assisted carrier hopping and electric field assisted carrier hopping [see Eq. (3) and text].

the range of 6–40 for our devices. This gives a mean free path in the range of 25–250 nm. Given the exceptionally weak electron-phonon coupling for acoustic phonons in nanotubes and graphite [18], we rule out phonon scattering as giving rise to this relatively short mean free path. One possibility for disorder on this length scale is atomic defects within each nanotube layer, taking the form of pentagon-heptagon defects that distort the local electronic structure. However, this possibility seems unlikely, given the straight, near-perfect appearance of the nanotube structure in high-resolution TEM studies. A second possibility is that layer-layer interactions between incommensurate layers gives rise to a disorder potential among otherwise atomically perfect nanotube layers. Indeed, it has been demonstrated in theoretical studies that atomic mismatch between otherwise defect-free shells can lead to diffusive transport along the axis of MWNTs [19].

Our transport results have important implications for the degree of phase coherence for charge carriers in tele-scoped MWNTs. First, the phenomena require that the phase coherence length,  $l_\phi$ , be larger than the diameter of the nanotube. In this sense, multiwall nanotubes are one-dimensional phase objects, independent of the dimensionality of band structure effects. Additionally, the nonlinear  $R(x)$  behavior observed here implies that the carriers maintain a degree of phase coherence between scattering events, and that the phase coherence length  $l_\phi$  at least approaches (and perhaps surpasses)  $l_c$ . The exact relationship implied between the phase coherence length and the localization length is not clear, mainly because the regime  $l_\phi \sim l_c$  is not theoretically well understood [20]. An unambiguous exponential length dependence would be a clear sign of  $l_\phi \gg l_c$ . However, the data presented here do not unambiguously *prove* an exponential relationship. Such proof typically demands data that vary over many decades. A general functional form of  $R(x)$  is not known, to our knowledge, in the regime of  $l_\phi \sim l_c$ . The exponential form probably persists as  $l_\phi$  is reduced, giving rise to other nonlinear forms for  $l_\phi \sim l_c$  (such as a power law as suggested above for our data), then eventually to a linear form for  $l_\phi \ll l_c$  (weak localization). However, even with conservative estimates, the phase coherence length is surprisingly long (perhaps as long as the nanotube itself), given that the experiments were performed at room-temperature. The unique properties of nanotubes (including low concentrations of defects, weak electron-phonon coupling, and unusual Debye temperature and screening length [18,21]) are most likely responsible for the implied long  $l_\phi$  values.

We thank K. Bradley, M. L. Cohen, S. Das Sarma, M. S. Fuhrer, D.-H. Lee, S. G. Louie, and E. Stach for helpful interactions. This work was supported by the Director, Office of Energy Research, Office of Basic Energy

Sciences, Division of Material Sciences, of the U.S. Department of Energy under Contract No. DE-AC03-76SF00098, and also NSF Grants No. CCR-0210176, No. EIA-0205641, and No. DMR-9801738.

---

\*Present Address: Department of Physics, Stanford University, Stanford, CA 94305, USA

†Corresponding Author, email: azettl@physics.berkeley.edu

- [1] C. T. White and T. N. Todorov, *Nature (London)* **393**, 240 (1998).
- [2] A. Bachtold *et al.*, *Phys. Rev. Lett.* **84**, 6082 (2000).
- [3] A. Javey *et al.*, *Nature (London)* **424**, 654 (2003).
- [4] A. Bachtold *et al.*, *Nature (London)* **397**, 673 (1999).
- [5] S. Frank *et al.*, *Science* **280**, 1744 (1998); C. Berger *et al.*, *Appl. Phys. A* **74**, 363 (2002); S. Sanvito *et al.*, *Phys. Rev. Lett.* **84**, 1974 (2000).
- [6] P. G. Collins *et al.*, *Phys. Rev. Lett.* **86**, 3128 (2001).
- [7] H. Dai, E. W. Wong, and C. M. Lieber, *Science* **272**, 523 (1996).
- [8] J. Cumings, P. G. Collins, and A. Zettl, *Nature (London)* **406**, 586 (2000).
- [9] J. Cumings and A. Zettl, *Science* **289**, 602 (2000).
- [10] J.-C. Charlier and J.-P. Michenaud, *Phys. Rev. Lett.* **70**, 1858 (1993); M.-F. Yu, B. I. Yakobson, and R. S. Ruoff, *J. Phys. Chem. B* **104**, 8764 (2000).
- [11] P. G. Collins and P. Avouris, *Appl. Phys. A* **74**, 329 (2002).
- [12] D.-H. Kim and K. J. Chang, *Phys. Rev. B* **66**, 155402 (2002); C. Buia, A. Buldum, and J. P. Lu, *Phys. Rev. B* **67**, 113409 (2003).
- [13] R. Landauer, *Philos. Mag.* **21**, 863 (1970); D. J. Thouless, *Phys. Rev. Lett.* **39**, 1167 (1977).
- [14] G. J. Dolan and D. D. Osheroff, *Phys. Rev. Lett.* **43**, 721 (1979); D. J. Bishop, D. C. Tsui, and R. C. Dynes, *Phys. Rev. Lett.* **44**, 1153 (1980); M. S. Fuhrer *et al.*, *Solid State Commun.* **109**, 105 (1999); Y. Koike *et al.*, *J. Phys. Soc. Jpn.* **54**, 713 (1985).
- [15] This theoretical model has also been implicated in recent measurements of nonlinear resistance in single-walled nanotubes [P. J. de Pablo *et al.*, *Phys. Rev. Lett.* **88**, 036804 (2002)].
- [16] S. Datta, *Electronic Transport in Mesoscopic Systems* (Cambridge University Press, New York, 1997), p. 199.
- [17] N. Apsley and H. P. Hughes, *Philos. Mag.* **31**, 1327 (1975).
- [18] Z. Yao, C. L. Kane, and C. Dekker, *Phys. Rev. Lett.* **84**, 2941 (2000).
- [19] S. Roche *et al.*, *Phys. Lett. A* **285**, 94 (2001).
- [20] P. A. Lee and T. V. Ramakrishnan, *Rev. Mod. Phys.* **57**, 287 (1985).
- [21] J. Hone, in *Carbon Nanotubes: Synthesis, Structure, Properties, and Applications*, edited by M. S. Dresselhaus, G. Dresselhaus, and P. Avouris (Springer-Verlag, Berlin, 2001), p. 273-286; F. Leonard and J. Tersoff, *Phys. Rev. Lett.* **83**, 5174 (1999).